

# Supporting Information

Hakulinen et al. 10.1073/pnas.1203971109

## SI Materials and Methods

**Expression and Purification of *Ilyobacter tartaricus* F<sub>1</sub>F<sub>o</sub> and F<sub>o</sub>.** WT *Ilyobacter tartaricus* F<sub>1</sub>F<sub>o</sub>-ATP synthase (ITF<sub>1</sub>F<sub>o</sub>) was expressed and purified as described by Neumann et al. (1). Recombinant ITF<sub>1</sub>F<sub>o</sub> was expressed in *Escherichia coli* DK8 cells (2) using plasmid pITr5Hisa with a His<sub>12</sub>-tag at the N terminus of the a-subunit in ZY505 medium (3) at 37 °C. Protein synthesis was induced at an OD<sub>600</sub> of 0.4–0.5 with 0.2 mM isopropyl thio-galactoside for 2 h. For ITF<sub>1</sub>F<sub>o</sub> purification, the membranes were isolated by sequential centrifugation and homogenized in 50 mM KPi at pH 7.0, 200 mM KCl, 10% (vol/vol) glycerol, 40 mM imidazole at pH 7.0, 2 mM MgCl<sub>2</sub>, and Pefablock (membrane buffer; Sigma–Aldrich Chemie GmbH) If *I. tartaricus* F<sub>o</sub> complex (ITF<sub>o</sub>) was purified, the isolated membranes were homogenized in 20 mM Tris-HCl at pH 8.0, 5 mM EDTA-K<sub>2</sub>-KOH at pH 8.0, 5% (vol/vol) glycerol, 1 mM DTT, and 3.5 M urea, and they were stirred at 4 °C for 30 min. The membranes were diluted to a urea concentration >0.3 M with 50 mM Tris-HCl at pH 8.0, collected by ultracentrifugation, and homogenized into membrane buffer without MgCl<sub>2</sub>. After solubilization in dodecyl-β-D-maltoside (DDM), the protein was purified by affinity chromatography on Ni<sup>2+</sup>-NTA resin (GE Healthcare). The pure ITF<sub>1</sub>F<sub>o</sub> or ITF<sub>o</sub> was concentrated in an ultrafiltration device (Millipore or Vivaspin), and the buffer was changed to 20 mM Tris-HCl at pH 8.0, 200 mM KCl, 1 mM MgCl<sub>2</sub> (F<sub>1</sub>F<sub>o</sub> only), and 1 mM DTT with an appropriate detergent on a desalting column (Thermo Scientific). The protein was stored at 4 °C or frozen in liquid nitrogen. If the protein was further purified or analyzed by size exclusion chromatography (directly after affinity chromatography), Superose 6 (3.2/30; GE Healthcare) was used in a buffer of 20 mM Tris-HCl at pH 8.0, 150 mM or 200 mM KCl, 1 mM DTT, and 2 mM MgCl<sub>2</sub> with an appropriate detergent.

**Purification of the ITF<sub>1</sub>F<sub>o</sub> and F<sub>o</sub> Samples for Laser-Induced Liquid Bead Ion Desorption MS.** ITF<sub>1</sub>F<sub>o</sub> (WT and recombinant) was subjected to size exclusion chromatography in a buffer of 20 mM Tris-HCl at pH 8.0, 150 mM KCl [WT ITF<sub>1</sub>F<sub>o</sub> (wtITF<sub>1</sub>F<sub>o</sub>)] or 200 mM KCl [recombinant ITF<sub>1</sub>F<sub>o</sub> (recITF<sub>1</sub>F<sub>o</sub>)], 1 mM DTT, 2 mM MgCl<sub>2</sub>, and 0.1% DDM before laser-induced liquid bead ion desorption (LILBID) MS to obtain better protein quality. ITF<sub>o</sub> was purified in 0.144% Cymal-7 on metal chelate affinity chromatography, and the buffer was changed to 20 mM Tris-HCl at pH 8.0, 150 mM KCl, 1 mM DTT, and 0.114% Cymal-7.

**LILBID-MS.** LILBID-MS was performed as described by Hoffmann et al. (4). All proteins were kept at 4 °C during sample preparation. Before measurement, wtITF<sub>1</sub>F<sub>o</sub>, recITF<sub>1</sub>F<sub>o</sub>, and ITF<sub>o</sub> samples were diluted to 1.1 mg/mL, 1.67 mg/mL, and 0.43 mg/mL, respectively, and desalted on Zeba Spin Columns 7K MWCO (Thermo Fisher Scientific) using 10 mM Tris-HCl buffer containing 0.05% DDM. For both ITF<sub>1</sub>F<sub>o</sub> variants, the ITF<sub>1</sub>F<sub>o</sub> from WT cells (1) and ITF<sub>1</sub>F<sub>o</sub> expressed in DK8, 1 mM MgCl<sub>2</sub> was added to the buffer. Data analysis was performed using homemade Labview software.

**Purification of Recombinant *I. tartaricus* F<sub>1</sub>F<sub>o</sub> with Additional Lipids.** Recombinant ITF<sub>1</sub>F<sub>o</sub> was solubilized in 1% Triton X-100 and washed after binding to Ni<sup>2+</sup>-NTA material with 50 mM KPi pH 8.0, 100 mM KCl, 2 mM MgCl<sub>2</sub>, 10% (vol/vol) glycerol, 25 mM Imidazol-HCl pH 8.0, 0.1% Triton X-100 (wash buffer 1) and with the same buffer containing 10 mM Imidazol-HCl pH 8.0 and 0.02% Triton X-100 (wash buffer 2). Subsequently an

incubation with 1 mg each 1-palmitoyl-2-oleoyl-*sn*-glycero-3-phosphocholine (POPC), 1-palmitoyl-2-oleoyl-*sn*-glycero-3-phosphoethanolamine (POPE) and 1-palmitoyl-2-oleoyl-*sn*-glycero-3-phospho-(1'-*rac*-glycerol) (POPG) homogenized in the wash buffer 2 was carried out for 4 h. The excess lipid was washed off with wash buffer 2 (~10 column volumes). The eluted ITF<sub>1</sub>F<sub>o</sub> was precipitated in 15% (wt/wt) polyethylene glycol (PEG) 6,000 for 1 h. The precipitated protein was pelleted by centrifugation at 19,000 × *g* for 30 min (4 °C) and homogenized into 10 mM Tris-HCl pH 8.0, 0.01% Triton X-100.

**Other Biochemical Methods.** The bicinchoninic acid method (Pierce) was used for protein concentration determination with BSA as a protein standard. For analysis of protein samples, 13.2% (vol/vol) SDS/PAGE was used, as described by Schägger and von Jagow (5). The gels were stained by silver staining according to the method of Nesterenko et al. (6). For Western blot analysis, the proteins were separated in SDS/PAGE and the gel was blotted on a 0.45-μm polyvinylidene difluoride membrane (Immobilon-P; Millipore) in a semidry blot system (Bio-Rad) using 25 mM Tris and 192 mM glycine as a transfer buffer at 15 V for 40 min. The unspecific binding sites were blocked in 5% milk powder, 20 mM Tris-HCl at pH 7.5, and 150 mM NaCl. The primary monoclonal mouse antipolyhistidine antibody and alkaline phosphate-conjugated IgG antibody (both from Sigma) were applied as a 1:1,000 dilution. The blot was stained using Sigma Fast BCIP/NBT alkaline phosphate substrate (Sigma–Aldrich Chemie GmbH). The hydrolysis activity of ATP synthase was investigated by a coupled spectrometric assay as described by Laubinger and Dimroth (7). The *I. tartaricus* membranes were prepared for lipid extraction as described by Neumann et al. (1). The lipid extraction followed the method of Folch et al. (8).

**Lipid Analysis by TLC.** The lipid analysis of protein samples was performed by TLC. A 10- to 60-μg sample was loaded on a silica gel plate (Merck), and lipids were separated with chloroform/methanol/water (39:15:2.4 ratio). If the lipids were separated in the second dimension, solvent with chloroform/methanol/ammonia (13:7:1 ratio) was used. The lipids were stained unspecifically with iodine vapor (9), phospholipids were stained with molybdenum blue (10), and ethanolamines were stained with ninhydrine (11).

**Atomic Force Microscopy.** An atomic force microscope equipped with a 100-μm XY piezo scanner (Nanoscope IIIa; DI/VEECO) was used for imaging, equipped with cantilevers (OMCL RC-800-PS; Olympus; 200-μm-long spring constant of 0.05 N/m). Samples from ITF<sub>o</sub> reconstitution setups were diluted to a final concentration of about 10–20 μg/mL and adsorbed onto freshly cleaved mica in an adsorption buffer [300 mM KCl, 25 mM MgCl<sub>2</sub>, 20 mM Tris-HCl (pH 7.0)] for 30 min and washed with an imaging buffer [150 mM KCl, 20 mM Tris-HCl (pH 7.0)] (12). The topographies were recorded at 25 °C at a maximal loading force of 100 pN and an optimized line scanning frequency of 5–7 Hz. Image processing was performed using Nanoscope v.5 and v.6 (DI/VEECO), BOXER from EMAN (13), IMAGIC (14), and ImageJ (National Institutes of Health) (15). Diameters of the oligomers were measured at full-width half-protrusion from the lipid bilayer, and particles were classified based on their stoichiometry determined in the raw images using Nanoscope v.6. Particles were selected for averaging using the BOXER manual particle picking procedure and further analyzed in IMAGIC.

**Immunogold on Grid Labeling.** Immunogold on grid labeling was performed as described by Kleymann et al. (16) and Ribrioux et al. (17) with following modifications. Samples were absorbed on nickel grids coated with polyform, carbon film, and 0.1% poly-L-lysine. The samples were treated with PBS at pH 7.4 (2 min), with 0.1% BSA in PBS (5 min) at room temperature, and with a 1:1,000 dilution of antihistidine antibody produced in mouse (Novagen) in 0.1% BSA and PBS at pH 7.4 (1 h). The samples were washed four times with PBS for 2 min and incubated with a 1:50 dilution of anti-mouse antibody from goat coupled with nanogold for 50 min. The unbound antibody was washed off with PBS (4 times for 5 min), and the samples were fixed with 1% glutaraldehyde in PBS for 5 min and washed three times in water for 5 min. The grids were stained with 1% (wt/wt) uranyl acetate and screened in a Philips CM208 microscope at an acceleration voltage of 40–100 kV. The images were recorded on a 1k × 1k CCD camera.

## SI Results

**Analysis of Purified ITF<sub>o</sub>.** The stability of the purified ITF<sub>o</sub> was investigated on SDS/PAGE and by Western blot analysis. The stoichiometry and the subunit composition of the purified ITF<sub>o</sub> were maintained over several months at 4 °C. In further investigations, the purified F<sub>o</sub> was mixed with POPC/1,2-dipalmitoyl-*sn*-glycero-3-phosphocholine lipid mixture and incubated for 23 d at room temperature (Fig. 1A). All the F<sub>o</sub> subunits were detected in the SDS/PAGE in the same stoichiometry as directly after purification (Fig. 1A). Analytical size exclusion chromatography with a Superose 6 (3.2/30) column was used for the analysis of ITF<sub>o</sub> assembly and dispersity. Using Cymal-5 as the detergent, the main peak eluted at 1.47 mL containing ITF<sub>o</sub> with subunits a and b, as well as the c<sub>11</sub> ring (Fig. S1B). Similar results were obtained with several other detergents, including maltosides and cymals. The results indicate that the purified ITF<sub>o</sub> is fully assembled and contains all its subunits, in agreement with LILBID-MS (Fig. 1).

**Lipid Analysis.** To crystallize the F<sub>o</sub> subcomplex in a 2D manner, the lipid composition of *I. tartaricus* whole-lipid extracts, of purified wtITF<sub>1</sub>F<sub>o</sub>, and of *E. coli* produced ITF<sub>1</sub>F<sub>o</sub> was investigated by TLC (Fig. S3). The lipid extraction from *I. tartaricus* cells was

performed as described by Folch et al. (8) and analyzed using TLC. The whole-lipid extract contained POPC (PC), POPG (PG), and POPE (PE) lipids and possibly cardiolipin (Fig. S3C). Two-dimensional TLC was applied to investigate whether phosphatidylserine lipids are present in the sample, because they run at the same height as PC (Fig. S3C). In addition to PC, PG, and PE lipids, two lipid spots were detected that were stainable with molybdenum blue but not with ninhydrine. The spots could represent cardiolipin. Purified wtITF<sub>1</sub>F<sub>o</sub> (1) binds PC, PG, PE, and an additional (unknown) lipid (18). Therefore, it was investigated whether ITF<sub>1</sub>F<sub>o</sub> expressed in *E. coli* and purified via affinity chromatography also binds these lipids. The wtITF<sub>1</sub>F<sub>o</sub> showed bound PC, PG, and PE lipids (Fig. S3A). In contrast, the recombinant ITF<sub>1</sub>F<sub>o</sub> did not show any bound lipids (Fig. S3A). To investigate whether the recombinant ITF<sub>1</sub>F<sub>o</sub> is able to bind these lipids, synthetic POPC, POPG, and POPE were added during the Ni<sup>2+</sup>-NTA purification procedure of a recombinant ITF<sub>1</sub>F<sub>o</sub> sample. After washing, elution, and PEG precipitation, POPC and POPG, and possibly a small amount of POPE, were still present at the recombinant ITF<sub>1</sub>F<sub>o</sub> (Fig. S3A, black arrow).

Taken together, the lipid analysis shows that *I. tartaricus* whole-lipid extract contains PG, PC, and PE lipids and probably cardiolipin. The wtITF<sub>1</sub>F<sub>o</sub> purified by PEG precipitation binds PG, PC, and PE lipids, whereas ITF<sub>1</sub>F<sub>o</sub> expressed in *E. coli* and purified via affinity chromatography does not bind any lipids. If synthetic POPG, POPC, and POPE lipids are provided during purification, the recombinant ITF<sub>1</sub>F<sub>o</sub> binds POPG and POPC, and perhaps a small amount of POPE.

## Secondary Structure and Topography Analysis of the *I. tartaricus* a-Subunit.

The *I. tartaricus* a-subunit (ITa) consists of 288 amino acids. An amino acid sequence alignment and topology analysis (Fig. S9) shows the presence of an N-terminal extension in ITa, which is not present in most other bacterial a-subunits. The extension is a predicted  $\alpha$ -helix (helix "0"). LILBID-MS (this work) and MALDI-MS (19) show that the ITa is neither posttranslationally modified nor cleaved in the native ATP synthase; thus, it presumably consists of 6 transmembrane helices. Consequently, the ITF<sub>o</sub> complex harbors 6 (a) + 2 (b<sub>2</sub>) + 22 (c<sub>11</sub>) = 30 transmembrane  $\alpha$ -helices, divided into 22 rotor and 8 stator helices.

- Neumann S, Matthey U, Kaim G, Dimroth P (1998) Purification and properties of the F<sub>1</sub>F<sub>o</sub> ATPase of *Ilyobacter tartaricus*, a sodium ion pump. *J Bacteriol* 180:3312–3316.
- Klionsky DJ, Brusilow WS, Simoni RD (1984) In vivo evidence for the role of the epsilon subunit as an inhibitor of the proton-translocating ATPase of *Escherichia coli*. *J Bacteriol* 160:1055–1060.
- Studier FW (2005) Protein production by auto-induction in high density shaking cultures. *Protein Expr Purif* 41:207–234.
- Hoffmann J, et al. (2010) ATP synthases: Cellular nanomotors characterized by LILBID mass spectrometry. *Phys Chem Chem Phys* 12:13375–13382.
- Schägger H, von Jagow G (1987) Tricine-sodium dodecyl sulfate-polyacrylamide gel electrophoresis for the separation of proteins in the range from 1 to 100 kDa. *Anal Biochem* 166:368–379.
- Nesterenko MV, Tilley M, Upton SJ (1994) A simple modification of Blum's silver stain method allows for 30 minute detection of proteins in polyacrylamide gels. *J Biochem Biophys Methods* 28:239–242.
- Laubinger W, Dimroth P (1987) Characterization of the Na<sup>+</sup>-stimulated ATPase of *Propionigenium modestum* as an enzyme of the F<sub>1</sub>F<sub>o</sub> type. *Eur J Biochem* 168:475–480.
- Folch J, Lees M, Sloane Stanley GH (1957) A simple method for the isolation and purification of total lipides from animal tissues. *J Biol Chem* 226:497–509.
- Gasser W, O'Brien J, Schwan D, Wilcockson D, Bitter P (1977) Lecithin/spingomyelin ratio procedure by thin-layer chromatography. *Am J Med Technol* 43:1155–1159.
- Müthing J, Radloff M (1998) Nanogram detection of phospholipids on thin-layer chromatograms. *Anal Biochem* 257:67–70.
- Hecht E, Mink C (1952) The methodology of the ninhydrin reaction and paper chromatography in connection with investigations of phosphatide of physiological interest in blood coagulation. *Biochim Biophys Acta* 8:641–653.
- Müller DJ, Engel A (1997) The height of biomolecules measured with the atomic force microscope depends on electrostatic interactions. *Biophys J* 73:1633–1644.
- Ludtke SJ, Baldwin PR, Chiu W (1999) EMAN: Semiautomated software for high-resolution single-particle reconstructions. *J Struct Biol* 128:82–97.
- van Heel M, Harauz G, Orlova EV, Schmidt R, Scharf M (1996) A new generation of the IMAGIC image processing system. *J Struct Biol* 116:17–24.
- Abramoff MD, Magelhaes PJ, Ram SJ (2004) Image processing with ImageJ. *Biophotonics International* 11:36–42.
- Kleymann G, et al. (1995) Immunoelectron microscopy and epitope mapping with monoclonal antibodies suggest the existence of an additional N-terminal transmembrane helix in the cytochrome b subunit of bacterial ubiquinol:cytochrome-c oxidoreductases. *Eur J Biochem* 230:359–363.
- Ribrioux S, et al. (1996) Use of nanogold- and fluorescent-labeled antibody Fv fragments in immunocytochemistry. *J Histochem Cytochem* 44:207–213.
- Meier T, Matthey U, Henzen F, Dimroth P, Müller DJ (2001) The central plug in the reconstituted undecameric c cylinder of a bacterial ATP synthase consists of phospholipids. *FEBS Lett* 505:353–356.
- Meier T, von Ballmoos C, Neumann S, Kaim G (2003) Complete DNA sequence of the *atp* operon of the sodium-dependent F<sub>1</sub>F<sub>o</sub> ATP synthase from *Ilyobacter tartaricus* and identification of the encoded subunits. *Biochim Biophys Acta* 1625:221–226.



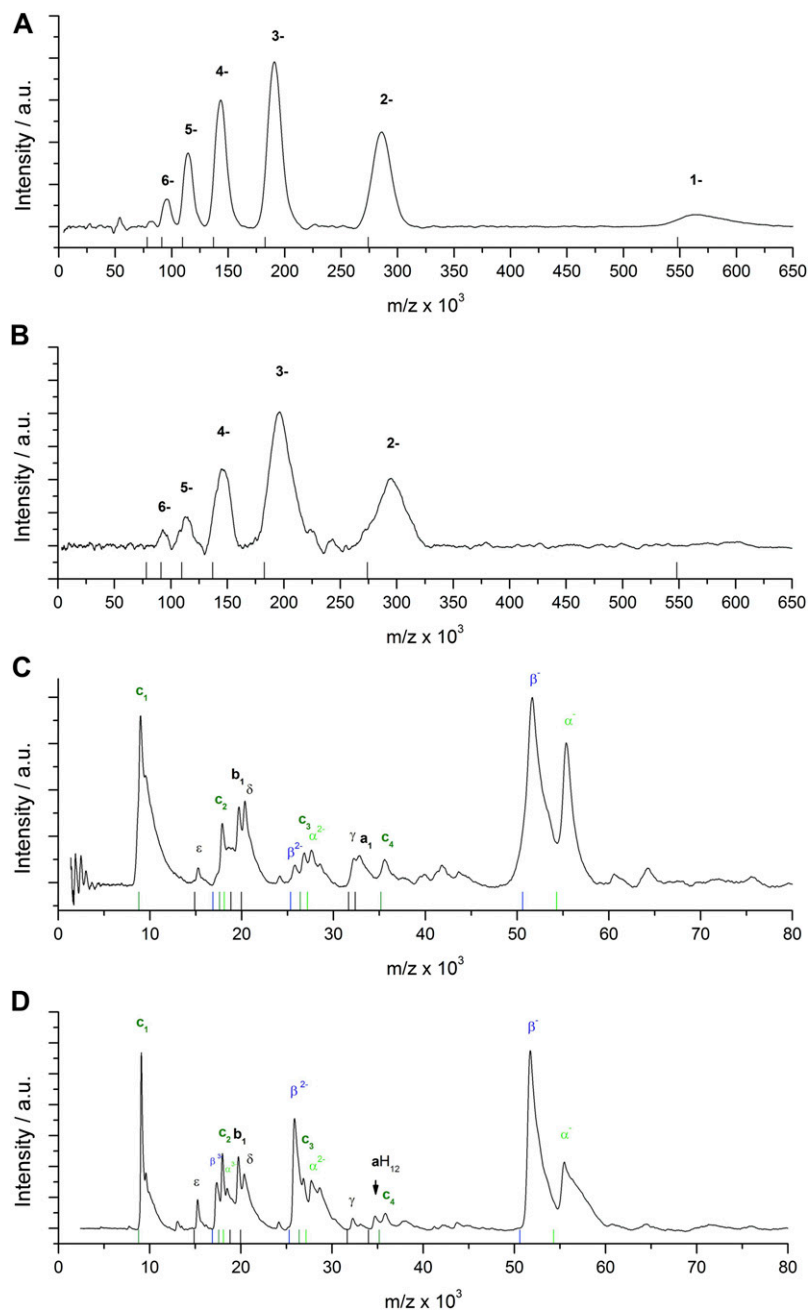


**Fig. S2.** MS analysis of ITF<sub>1</sub>F<sub>o</sub> by LILBID-MS. (A) wtITF<sub>1</sub>F<sub>o</sub>, low laser intensity. (B) ITF<sub>1</sub>F<sub>o</sub> heterologously expressed in *E. coli* cells, low laser intensity. (C) wtITF<sub>1</sub>F<sub>o</sub>, high laser intensity. (D) ITF<sub>1</sub>F<sub>o</sub> heterologously expressed in *E. coli* cells, high laser intensity. The charged states (1– to 6–) of ITF<sub>1</sub>F<sub>o</sub> and the single subunits (and some complexes) are indicated by bars (x axis represents theoretically expected masses) and labels. a.u., arbitrary unit.





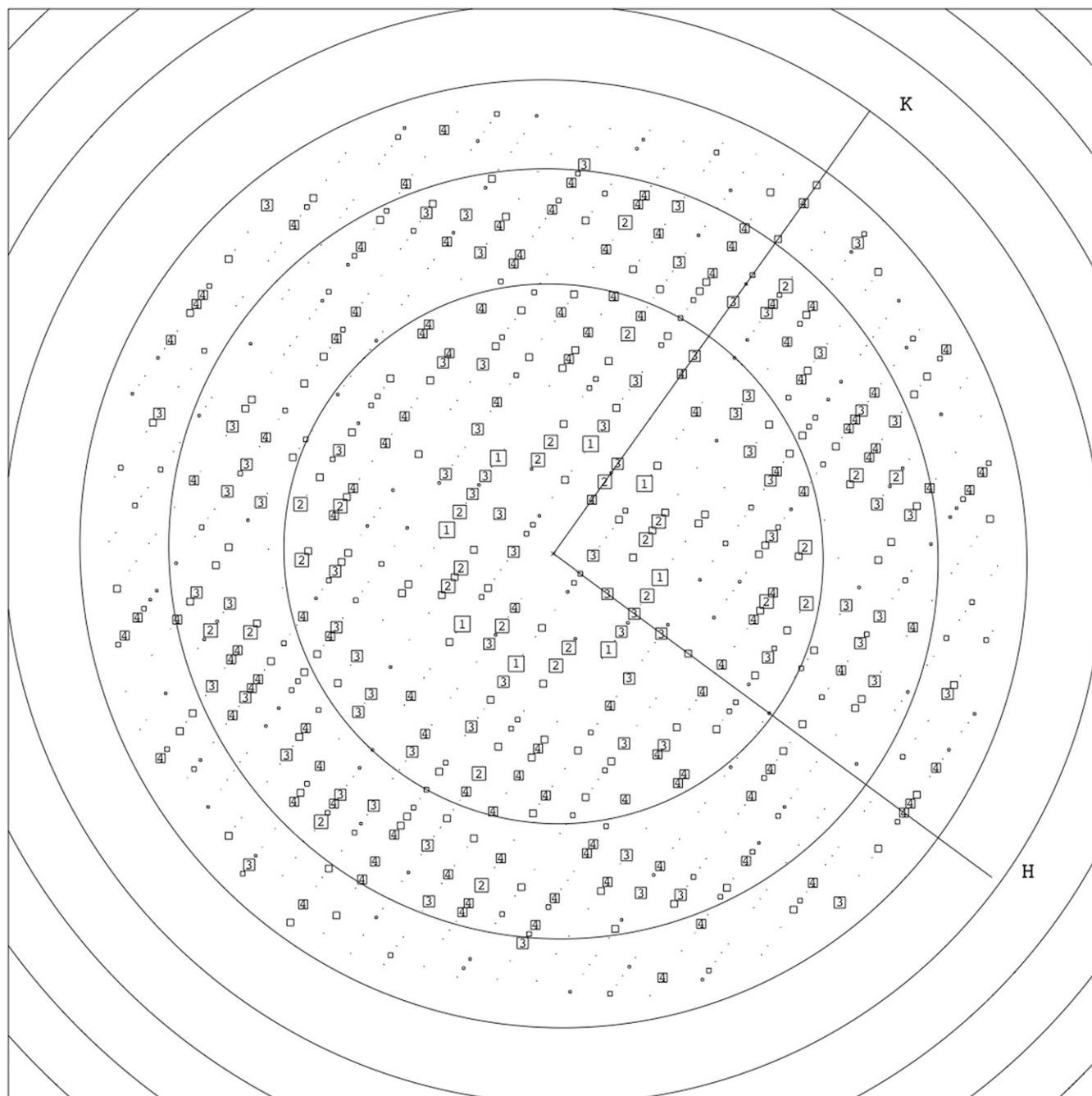


**Fig. 54.** Calculated Fourier transform of a single crystal with a unit cell measuring  $81 \text{ \AA} \times 252 \text{ \AA}$ . The signal-to-noise ratio [image quality (IQ) values] of the spots is shown as squares and numbers in the reciprocal lattice (1). The largest box size and smallest number indicate the strongest reflections. The zero crossings of the contrast transfer function are indicated as concentric rings. The edge of the box represents  $5 \text{ \AA}$ . H, K: Miller indices.

1. Henderson R, Baldwin JM, Downing KH, Lepault J, Zemlin F (1986) Structure of purple membrane from *Halobacterium halobium*: Recording, measurement and evaluation of electron micrographs at  $3.5 \text{ \AA}$  resolution. *Ultramicroscopy* 19:147–178.

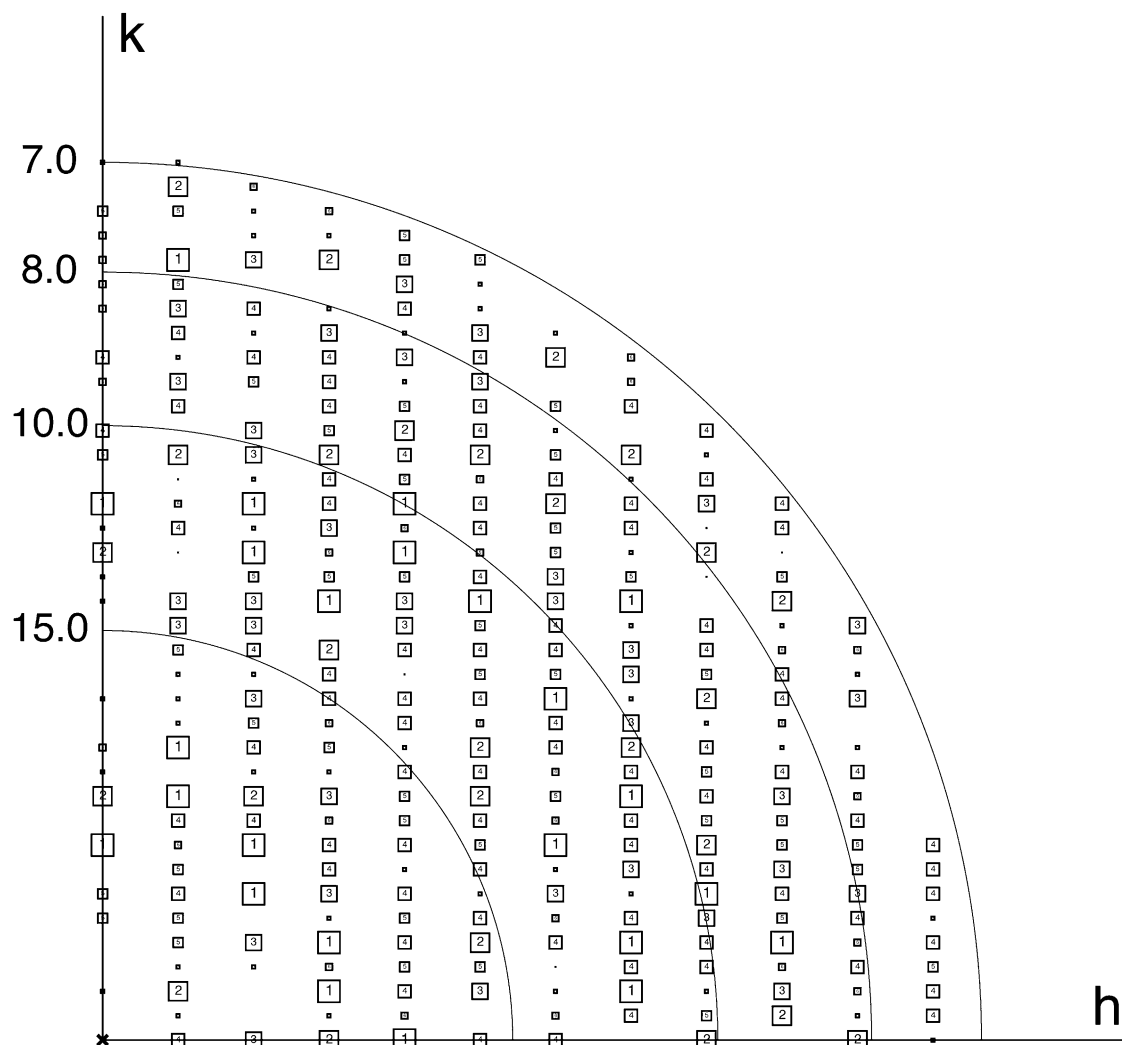
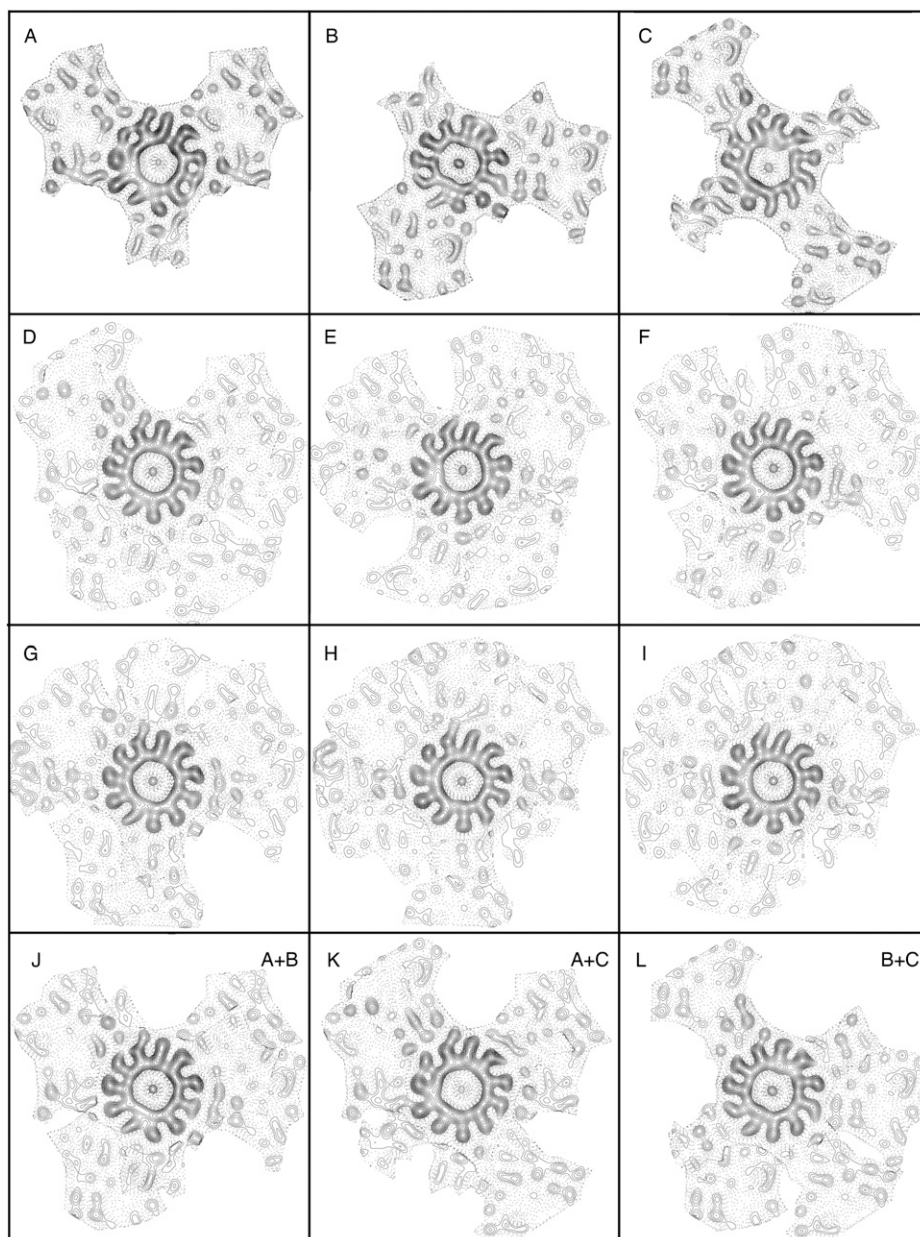


Fig. S5. Combined phase error after merging five crystals to 7.0 Å. The error associated with each measurement is indicated in the box size (1 < 8°, 2 < 14°, 3 < 20°, 4 < 30°, where 90° is random). Decreasing box size shows higher values, and values from 1 to 4 are shown as numbers. h, k: Miller indices.







**Fig. S7.** Noncrystallographic symmetry averaging of the six different possible arrangements of *I. tartaricus*  $c_{11}$  and the extra densities. The asymmetrical unit of  $p12_1$  crystals has three different  $c_{11}$  rings, with neighboring extra densities as shown in Fig. S6. (A–C) Each ring in the asymmetrical unit with all surrounding densities (excluding the neighboring rings) was contoured. The contoured areas were rotated in such a way that the adjacent density to each ring would overlap, according to the six possible assignments shown in Fig. S6, and then aligned accurately to the nearest  $c$ -subunit only. Images aligned for Fig. S6A, as averaged in *D*, are shown in A–C. (D–I) Results of the averaging for the six different possibilities are shown in the same order as in Fig. S6. In all the six possibilities, the  $c$ -ring densities were enhanced, but only in one (*D*) were the extra densities increased as indicated by the higher number of contour levels. (J–L) Extra densities aligned for *D* averaged in pairs as indicated.

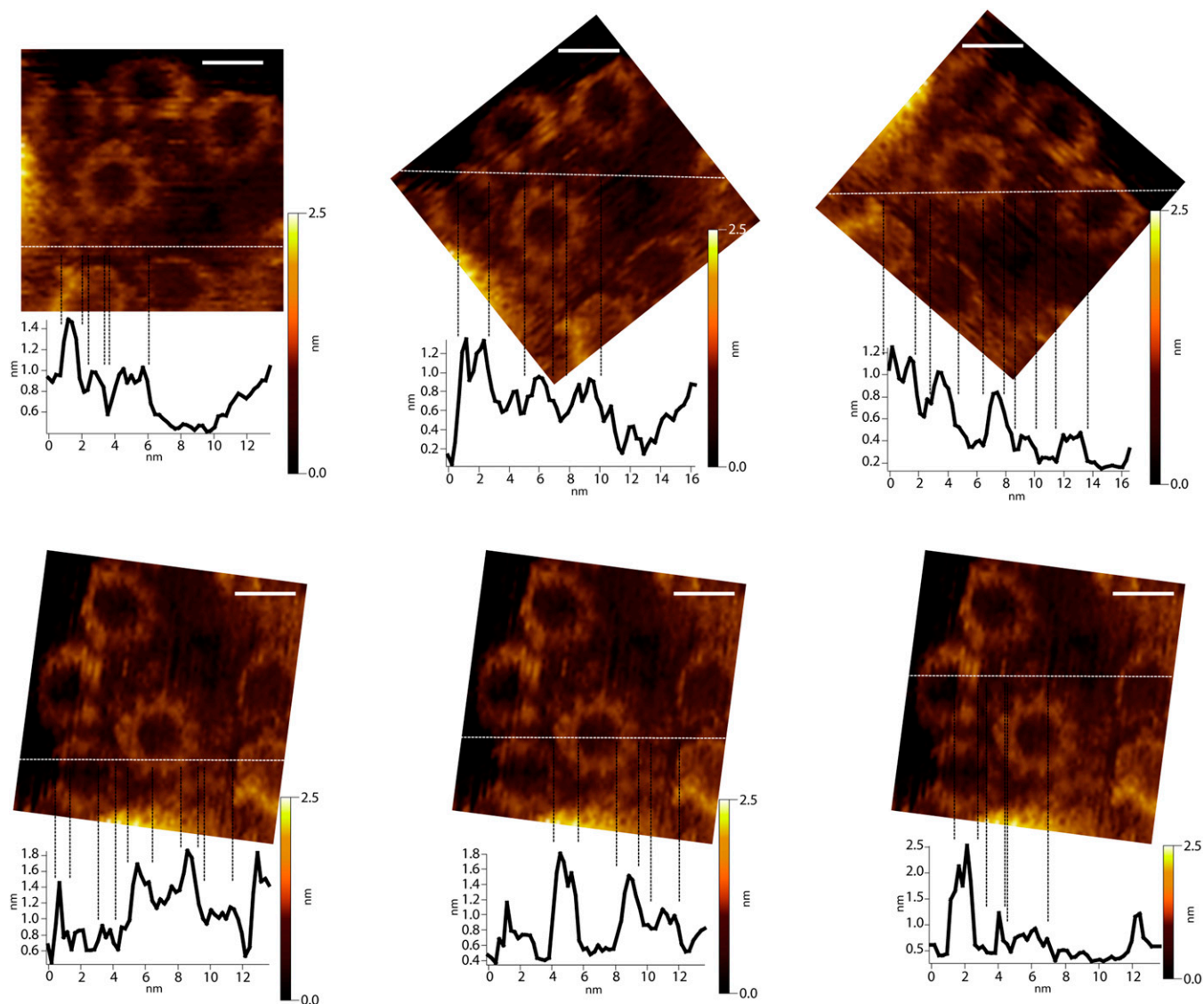


**Fig. S8.** Analysis of atomic force microscopy (AFM) topographs. Cross-sections of the AFM topographs illustrating height differences between the c-rings and the additional densities surrounding them. The average c-ring height above the lipid bilayer was  $0.7 \pm 0.1$  nm ( $n = 20$ ), and the height of the additional densities equaled  $0.4 \pm 0.1$  nm ( $n = 23$ ). The white dotted lines show the cross-section plane, and the black dotted lines link the features visible in the topograph and their cross-sections presented by the graphs. (Scale bars: 5 nm.) A color-coded height scale bar is given.

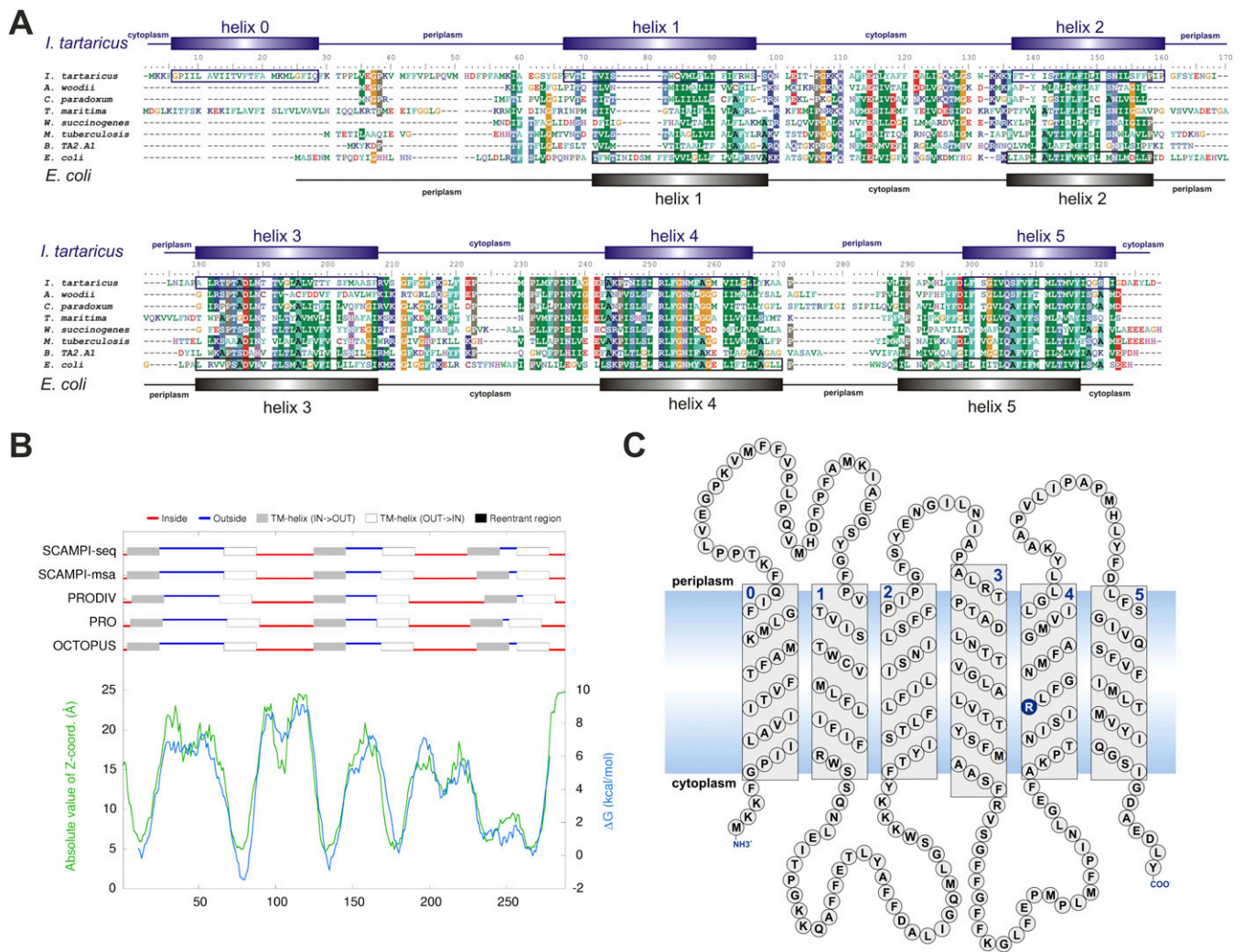


**Fig. S9.** *In silico* analysis of the *I. tartaricus* ATP synthase a-subunit. (A) Alignment of a-subunit sequences from F-type-ATP synthases of selected bacterial species. The individual sequences were aligned with the software BioEdit (<http://www.mbio.ncsu.edu/BioEdit/bioedit.html>). The following species are shown: *I. tartaricus*, *Acetobacterium woodii*, *Clostridium paradoxum*, *Thermotoga maritima*, *Wolinella succinogenes*, *Mycobacterium tuberculosis*, *Bacillus* sp. strain TA2.A1 (*Caldalkalibacillus thermarum* strain TA2.A1), and *E. coli*. The secondary structure elements for *E. coli* a-subunit are given in black according to Zhang and Vik (1). The corresponding regions for ITa are indicated in blue. A possible additional  $\alpha$ -helix at the N terminus of the ITa sequence is indicated as “helix 0.” (B) Prediction of transmembrane helices of ITa from amino acid sequence analysis with TOPCONS (2). Six transmembrane helices are predicted, but the N-terminal helix (helix 0) is not found in the *E. coli* a-subunit sequence. Z-coord., z coordinate. (C) Topology model of ITa based on the prediction by SOSUI (3) and experimental data (4, 5). A functional arginine 226 (blue, in helix 4) is essential for the *I. tartaricus* ATP synthase and plays a crucial role in the Na<sup>+</sup>-ion translocation through the F<sub>o</sub> complex (6).

- Zhang D, Vik SB (2003) Helix packing in subunit a of the *Escherichia coli* ATP synthase as determined by chemical labeling and proteolysis of the cysteine-substituted protein. *Biochemistry* 42:331–337.
- Bernsel A, Viklund H, Hennerdal A, Elofsson A (2009) TOPCONS: consensus prediction of membrane protein topology. *Nucleic Acids Res* 37:W465–468.
- Hirokawa T, Boon-Chieng S, Mitaku S (1998) SOSUI: classification and secondary structure prediction system for membrane proteins. *Bioinformatics* 14:378–379.
- Vorburger T, et al. (2008) Arginine-induced conformational change in the c-ring/a-subunit interface of ATP synthase. *FEBS J* 275:2137–2150.
- Daley DO, et al. (2005) Global topology analysis of the *Escherichia coli* inner membrane proteome. *Science* 308:1321–1323.
- Wehrle F, Appoldt Y, Kaim G, Dimroth P (2002) Reconstitution of F<sub>o</sub> of the sodium ion translocating ATP synthase of *Propionigenium modestum* from its heterologously expressed and purified subunits. *Eur J Biochem* 269:2567–2573.

**Table S1. Calculated\* and experimental masses of ITF<sub>1</sub>F<sub>o</sub> and F<sub>o</sub> complex measured by LILBID-MS**

Complex/subunits	<i>I. tartaricus</i> , WT		<i>I. tartaricus</i> expressed in <i>E. coli</i> DK8 cells	
	Calculated mass <sup>†</sup> , Da	LILBID mass, kDa	Calculated mass <sup>†</sup> , Da	LILBID mass, kDa
F <sub>1</sub> F <sub>o</sub> ( $\alpha_3\beta_3\gamma\delta\epsilon ab_2c_{11}$ )	548,052.7	548 ± 5	549,698.3	548 ± 5
F <sub>o</sub> (ab <sub>2</sub> c <sub>11</sub> )			168,397.8	168 ± 2
a	32,365.04	32.6 ± 0.3		
aHis <sub>12</sub>			34,010.72	34 ± 0.3 <sup>‡</sup>
b	18,821.88	18.6 ± 0.2	18,821.88	18.6 ± 0.2
c	8,794.85	8.8 ± 0.1	8,794.85	8.8 ± 0.1
$\alpha$	54,316.53	55.5 ± 0.5	54,316.53	55.5 ± 0.5
$\beta$	50,614.85	51 ± 0.5	50,614.85	51 ± 0.5
$\gamma$	31,657.62	32 ± 0.3	31,657.62	32 ± 0.3
$\delta$	19,961.36	19.5 ± 0.2	19,961.36	19.5 ± 0.2
e	14,887.38	14.8 ± 0.2	14,887.38	14.8 ± 0.2

\*As determined by Meier et al. (1) and Vorbürger et al. (2).

<sup>†</sup>Calculations were performed with BioEdit (<http://www.mbio.ncsu.edu/BioEdit/bioedit.html>) and do not include potential posttranslational modifications.

<sup>‡</sup>From F<sub>o</sub> sample.

1. Meier T, von Ballmoos C, Neumann S, Kaim G (2003) Complete DNA sequence of the *atp* operon of the sodium-dependent F<sub>1</sub>F<sub>o</sub> ATP synthase from *Ilyobacter tartaricus* and identification of the encoded subunits. *Biochim Biophys Acta* 1625:221–226.
2. Vorbürger T, et al. (2008) Arginine-induced conformational change in the c-ring/a-subunit interface of ATP synthase. *FEBS J* 275:2137–2150.